

CC bonds and (2) the strengthening effect on adjacent CC bonds is little affected by substitution of a second fluorine on the neighboring carbon atom. A similar pattern of the effect of fluorine substitution has been found for the CC force constants for the sequence of cyclopropenes, C_3H_4 , $\overline{CF_2-CH=CH}$, $\overline{CF_2-CF=CH}$, and $\overline{CF_2-CF=CF}$.⁵

West and co-workers assigned five of the six in-plane frequencies of $C_3Cl_3^+$ as observed in the infrared and Raman spectra of this ion.¹² They also studied the $C_3Br_3^+$ ion but were only able to obtain an infrared spectrum and to assign only two of this ion's fundamentals. A five-parameter Urey-Bradley potential function was fitted to the frequencies of the in-plane modes of the $C_3Cl_3^+$ ion. This potential function included a force constant for the nonbonded gem C...Cl interaction. When a small, but fixed value for a sixth constant, the nonbonded cis Cl...Cl interaction, was added, most of the other five force constants changed appreciably. Such high sensitivity of the calculation to a small modification implies a rather unstable numerical system and suggests being cautious in interpreting the results. Nonetheless, we shall compare West and co-workers' Urey-Bradley value of 6.31 mdyne/Å with our valence force field values of 7.87 for $C_3H_3^+$ and 7.71 for $C_3F_3^+$. To do so we must take account of the contributions of the nonbonded F_{CCl} force constants.²² This raises the Urey-Bradley value of 6.31 to a valence field value of 7.77, which is close enough to the values for $C_3H_3^+$ and $C_3F_3^+$ to imply that no appreciable

change occurs in the CC bond strength when the cyclopropenyl cation is fully substituted with chlorine or fluorine atoms.

Conclusions

A complete assignment of the eight vibrational fundamentals of the perfluorocyclopropenyl cation has been proposed. Normal-coordinate calculations with a selective overlay procedure for the three ions, $C_3FH_2^+$, $C_3F_2H^+$, and $C_3F_3^+$, gives a set of CC stretching force constants that conforms to the pattern found for fluorine substitution in cyclopropane and cyclopropene ring systems. Substitution of fluorine on a contiguous carbon atom increases the CC force constant, whereas substitution of a fluorine atom on a cross-ring carbon atom decreases the CC force constant. These effects are substantial and are presumed to correlate with bond-strength changes. In $C_3F_3^+$ the effect of fluorine substitution cancels out; the CC force constant is essentially the same as that in $C_3H_3^+$.

Confirmation and interpretation of these effects of fluorine substitution must await ab initio electronic calculations. Geometric parameters and force constants would be of interest as well as changes in electron densities as a function of fluorine substitution.

Acknowledgments. We are grateful to the donors of the Petroleum Research Fund, Administered by the American Chemical Society, Research Corporation, and the National Science Foundation (PRM-7911202 and PRM-81145415) for support of this research. We also appreciate Philip L. Steiner's contributions to the infrared experiments.

(22) Overend, J.; Scherer, J. R. *J. Chem. Phys.* 1960, 32, 1289-95.

Measurement of the Dissociation Energies of Gas-Phase Neutral Dimers by a Photoionization Technique: Values for *trans*-2-Butene/Sulfur Dioxide, (*trans*-2-Butene)₂, and Benzene/Sulfur Dioxide

J. R. Grover,* E. A. Walters,*† J. K. Newman,†† and M. G. White

Contribution from the Department of Chemistry, Brookhaven National Laboratory, Upton, New York 11973. Received January 22, 1985

Abstract: A method has been developed for the measurement of the dissociation energies of gas-phase neutral dimers using photoionization spectra of mass selected ions from molecular beams generated by jet expansion. This measurement involves the determination of the appearance potential for dissociative photoionization of the dimer using a difference technique. The 0 K dissociation energies obtained are 3.85 ± 0.23 , 2.9 ± 1.1 , and 4.40 ± 0.28 kcal/mol for *trans*-C₄H₈SO₂, (*trans*-C₄H₈)₂, and C₆H₆SO₂, respectively. The method is applicable for dimers in which the photoionization efficiency function of the partner of lower ionization potential begins with a distinct step at threshold, a condition that is satisfied for many molecules. The technique is best for heterodimers and less good for homodimers. At its best the experimental work can be accomplished within a day for a given dimer, and the data can be analyzed unambiguously in a model-independent fashion.

The universal long-range attraction of molecules for each other plays such a pivotal role in chemistry that chemists have made extraordinary efforts to understand the forces involved. Examples of such work are studies of virial coefficients,¹ infrared spectroscopy at elevated gas pressures,² and scattering in crossed molecular beams.³ Of special importance are the properties of weak complexes in the gas phase. With the advent of nozzle expansion techniques for their synthesis in molecular beams,⁴ and the introduction of laser fluorescence⁵ and dissociation,^{6,7} and microwave resonance methods⁸ for their investigation, the spectroscopic ex-

amination of weak complexes has achieved impressive elegance and power, and is now being enthusiastically pursued in several

(1) J. O. Hirschfelder, C. F. Curtiss, and R. B. Bird, "Molecular Theory of Gases and Liquids", Wiley, New York, 1954.

(2) R. J. LeRoy and J. S. Carley, *Adv. Chem. Phys.*, **42**, 353-420 (1980).

(3) (a) J. P. Toennies, "Physical Chemistry, An Advanced Treatise", Vol. VIA, W. Jost, Ed., Academic Press, New York, 1974, pp 227-381; (b) J. P. Toennies, *Annu. Rev. Phys. Chem.*, **27**, 225-260 (1976); (c) U. Buck, *Adv. Chem. Phys.*, **30**, 313-388 (1975).

(4) (a) P. G. Bentley, *Nature (London)*, **190**, 432-433 (1961); (b) W. Henkes, *Z. Naturforsch., Teil A*, **16**, 842 (1961); (c) N. Lee and J. B. Fenn, *Rev. Sci. Instrum.*, **49**, 1269-1272 (1978), and references therein; (d) ref 25 and references therein; (e) O. F. Hagena, "Molecular Beams and Low Density Gas Dynamics", P. P. Wegener, Ed., Marcel Dekker, New York, 1974, pp 93-181.

(5) (a) D. H. Levy, *Adv. Chem. Phys.*, **47**, 323-362 (1981); (b) R. E. Smalley, L. Wharton, and D. H. Levy, *Acc. Chem. Res.*, **10**, 139-145 (1977).

* Chemistry Department, University of New Mexico, Albuquerque, NM 87131.

† Participant in the National Synchrotron Light Source/High Flux Beam Reactor (NSLS/HFBR) Faculty-Student Support Program at Brookhaven National Laboratory.

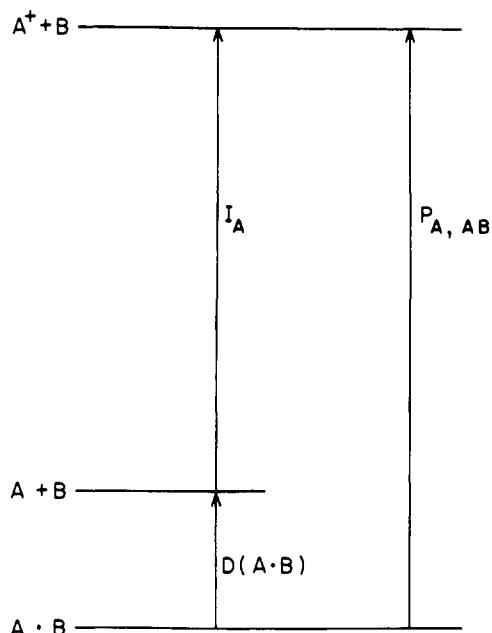


Figure 1. Energy diagram showing the relationship between the ionization potential I_A , the appearance potential $P_{A,AB}$, and the dissociation energy $D(A \cdot B)$.

laboratories. It is most exciting that structural details are now being obtained on complex polyatomic systems of chemical significance. However, one crucial area has remained weak, measurement of the energies of dissociation of the complexed molecules.

Such measurements have been made by equilibrium⁹ and spectroscopic^{6,10} techniques, but are nearly always laborious, and rely on special properties of the reagents or require case-by-case spectral analyses giving results that are not always unambiguous. In many instances estimates of unmeasured quantities are needed, or models must be invoked, to interpret the data. In consequence, only a few accurate energies of dissociation have been measured. We report here a photoionization technique for measuring with useful accuracy the energy of dissociation of neutral weak complexes in the gas phase that should be commonly applicable, and that is proving to be fast and unambiguous.

In this technique, photoionization data are used to obtain the dissociation energy $D(A \cdot B)$ of a target complex $A \cdot B$, where A is the moiety of lower ionization potential, via subtraction of the ionization potential I_A of A from the appearance potential $P_{A,AB}$ of A^+ from $A \cdot B$, as given in eq 1 and illustrated in Figure 1.

$$D(A \cdot B) = P_{A,AB} - I_A \quad (1)$$

Photoionization methods for measuring I_A are, of course, well known (a review is presented in ref 11, pp I-5 to I-34). The key is to find a good way to measure $P_{A,AB}$, because in the molecular beams formed by jet expansion $A \cdot B$ is only found in the presence of much larger amounts of uncombined A and B . In particular,

(6) M. A. Hoffbauer, C. F. Giese, and W. R. Gentry, *J. Phys. Chem.*, **88**, 181-184 (1984), and references therein.

(7) T. E. Gough, R. E. Miller, and G. Scoles, *J. Chem. Phys.*, **69**, 1588-1590 (1978).

(8) (a) T. Dyke, B. J. Howard, and W. Klemperer, *J. Chem. Phys.*, **56**, 2442-2454 (1972); (b) T. J. Balle, E. J. Campbell, M. R. Keenan, and W. H. Flygare, *Ibid.*, **72**, 922-932 (1980); (c) A. C. Legon, *Annu. Rev. Phys. Chem.*, **34**, 275-300 (1983).

(9) (a) M. Tamres, "Molecular Complexes", Vol. 1, R. Foster, Ed., Crane, Russak and Co., New York, 1973, pp 49-116; (b) M. Tamres and R. L. Strong, "Molecular Association", Vol. 2, R. Foster, Ed., Academic Press, New York, 1979, pp 331-456.

(10) Examples are: (a) J. A. Blazy, B. M. DeKoven, T. D. Russell, and D. H. Levy, *J. Chem. Phys.*, **72**, 2439-2444 (1980); (b) W. G. Read, E. J. Campbell, and G. Henderson, *Ibid.*, **78**, 3501-3508 (1983).

(11) H. M. Rosenstock, K. Draxl, B. W. Steiner, and J. T. Herron, *J. Phys. Chem. Ref. Data*, **6**, Suppl. No. 1, (1977).

the photoionization efficiency as a function of photon energy for the production of A^+ from such a mixture is dominated by the production of A^+ from A , with only a small contribution of A^+ from $A \cdot B$. Our strategy is to make an ancillary measurement of the photoionization efficiency for the production of A^+ from a beam of A containing no $A \cdot B$ but otherwise as nearly as possible under the same experimental conditions. The latter spectrum is then carefully normalized to that portion of the first spectrum that represents only the production of A^+ from A . Subtraction of the two spectra gives a difference spectrum that is the photoionization efficiency curve for the production of A^+ from $A \cdot B$ alone. The threshold of this difference spectrum represents the necessary value of $P_{A,AB}$. Of course, this simple strategy is complicated by the unavoidable presence of $A \cdot A$, trimers, etc., the minimization of or correction for which must be part of a complete prescription.

Experimental Section

The experiments reported here utilized the tunable photon beams available at line U11 of the 750-MeV storage ring at the National Synchrotron Light Source. A molecular beam containing the complex to be studied intersects the photon beam in the ion-extraction zone of a quadrupole mass spectrometer equipped with a channeltron detector operated in the ion counting mode. The intensity of the product ions of selected mass-to-charge ratio is measured as a function of photon wavelength. The relative photon intensity is measured simultaneously with a sodium salicylate screen-photomultiplier tube combination, enabling relative cross sections to be obtained. A more complete description of this apparatus and examples of its use are presented in ref 12. For the present work, an osmium-coated laminar grating¹³ of 1200-lines/mm groove density and 200-Å groove depth was used. The monochromator so equipped delivers usable light from 450 to 4500 Å. As measured using a calibrated photodiode, intensities are 2×10^{12} , 3×10^{12} , and 7×10^{12} photons/s at 584, 1000, and 1400 Å under typical conditions of 3-Å bandwidth and 100 mA of circulating electron current in the ring. The large bandwidth of 3 Å was used to achieve the high total counts necessary in these experiments. For all of the work reported here, except mass spectral scans at 584 Å, a 0.2-cm thick LiF filter was used to eliminate second and higher order radiation.

Molecular beams containing the complexes were produced by expansion of suitable gas mixtures through a 100-μm nozzle. The compositions and pressures of the mixtures were chosen to maximize signal strength and minimize contributions from clusters other than the complex of interest, as described below. Molecular beams containing reagent A only, without complexes, were easily achieved at lower nozzle pressures, often using neat gaseous A .

Success with the requisite subtractions of one spectrum from another demands that the spectra be measured to adequately high precision, which means that large numbers of total counts per photon energy bin must be accumulated to overcome scatter due to the statistics of counting. Thus, long runs are required and this makes the time stability of the system important if systematic errors are to be avoided. Three important instabilities were encountered. (1) The electron orbit position in the storage ring differs from fill to fill. This causes a corresponding shift in wavelength calibration from fill to fill because in the monochromator being used here¹⁴ there is no separate entrance slit; i.e., the stored electron beam itself is used as both light source and entrance slit, in order to achieve the largest possible photon intensities. Normally, each spectrum requires several fills to build up sufficient total counts, and these data must be summed in such a way that the wavelength bins are always accurate. This problem is easily solved if the spectrum of A^+ from A has a conspicuous threshold or feature of known wavelength that allows the wavelength scale to be calibrated before the spectra are summed. In the work reported here, this is always the case because the threshold of A (*trans*-2-butene $\equiv t\text{-C}_4\text{H}_8$ or benzene) has the form of an abrupt step. In several series, each of several runs (one run per fill), typical maximum corrections of 0.5 to 2 Å were encountered. All corrections were made to the nearest 0.1 Å, and since the data points were taken at 1-Å intervals, interpolation is necessary, where the interpolated points retain the same statistical significance as the raw data. Each interpolated point was therefore calculated from a simple cubic fit to four adjacent data points, usually two above and two below. (2) The sodium salicylate fluorescent

(12) M. G. White and J. R. Grover, *J. Chem. Phys.*, **79**, 4124-4131 (1983).

(13) A. Franks, K. Lindsey, J. M. Bennett, R. J. Speer, D. Turner, and D. J. Hunt, *Philos. Trans. R. Soc. London, Ser. A*, **277**, 503-543 (1975).

(14) M. R. Howells, *Nucl. Instrum. Methods*, **195**, 215-222 (1982).

screen plus photomultiplier combination used for the light monitor undergoes wavelength-dependent changes in efficiency rapidly enough that the difference spectra are sometimes significantly affected. (Recall that the ion intensity is divided by the light intensity at each point to provide a quantity proportional to cross section. It is the difference in effective cross sections that is wanted.) To solve this problem, a calibrated dc voltage proportional to the electron current circulating in the storage ring was used. The spectra to be subtracted are put in the form (ion intensity per unit ring current), and the resulting difference is then divided by the function (photon intensity per unit ring current). The remaining error due to the above-mentioned change in fluorescence efficiency is negligible. (3) The lithium fluoride filter undergoes wavelength-dependent changes in transmission near its cutoff wavelength at about 1050 Å while in use. This problem cannot be solved in the same way as the fluorescent screen problem described above, but can be mitigated by measuring the spectra of the dimer-containing beam and monomer reference beam alternately through several cycles. Our attempt to measure the dissociation energy for ethylene dimer was seriously hindered by this effect, but the measurements on the three title complexes were essentially unaffected because they were carried out at wavelengths much longer than 1050 Å. A measurement method that obviates the LiF filter has been devised and successfully tested, and will be described in a future report.

A small correction to all the spectra is made for scattered light. With the LiF filter in place the scattered light can be directly measured below 1030 Å, and its absorption by the filter can be measured below 450 Å, where no direct radiation remains. The shape of the scattered light intensity function at 1050 to 1400 Å is then estimated by extrapolation of the known function at 500 to 1030 Å. Finally, the scattered light is accurately proportional to the ring current, which provides an unambiguous basis for calculation of the correction at every wavelength.

The gas mixtures supplied to the nozzle must be time-stable in composition. On-line mixing in flow systems proved to be unsatisfactory. Two methods are adequate. When both or all reagents are gaseous and reasonably unreactive at room temperature and pressures of up to a few atmospheres, they are premixed in accurately measured proportions and stored in large stainless steel tanks until used (within a few hours). This was done, for example, with *trans*-2-butene and sulfur dioxide. When one reagent is a liquid of reasonably high vapor pressure at room temperature and the other is a gas that is unreactive with it, a bubbler is used. In our bubbler, the gas is forced through a glass frit a few centimeters below the surface of the liquid; the liquid volume and head volume are comparable, about 100 cm³. The head pressure, monitored with a capacitance manometer, is manually maintained at 800 torr with a precision of ± 5 torr. For both methods the nozzle pressure is electronically controlled to ± 1 torr or better at any desired value, usually ≤ 700 torr. All work reported here was done at the room temperature of 23 °C, which varied less than ± 1 °C. Beam conditions were usually sufficiently stable to carry out measurements within 5 min after startup for the premixed gases, and within 30 min for the bubbler.

Optimum conditions of gas composition and nozzle pressure must be separately determined for each case studied. In the following section we describe in detail how this was done for one example, *t*-C₄H₈ + SO₂. The object of the optimization is to produce a beam containing as large a proportion of A·B as possible, while keeping the proportions of A·A, the trimers A₃, A₂B, AB₂, and analogous larger clusters to sufficiently low levels, as established for each case. As the nozzle pressure is increased so that the temperature of the expanded gas decreases, the first clusters to become dominant are the dimers, followed by the trimers, tetramers, etc. This phenomenon gives rise to the familiar pattern in which the intensity of ions derived principally from dimers rises, maximizes, and falls while the intensity of ions derived from the competing trimers are rising strongly; the trimer-derived ions are dominated in turn by tetramer-derived ions, and so on. Fragmentation during the detector ionization process complicates this pattern for clusters comprised of polyatomic molecules, but it remains broadly valid, nevertheless. All of the foregoing matters have been extensively discussed in the literature.^{4c-e,5a,b} The most obvious way to avoid interference from trimers and larger clusters is therefore to work at sufficiently small nozzle pressures that they are not formed to a significant extent. On the other hand, for the difference experiment described here it is important to obtain as large an intensity of A⁺ from A·B as possible, and this means that the nozzle pressure must be chosen to be just below the point that A⁺ from trimers becomes troublesome. The required optimization can be done via measurements of the photoionization mass spectra of beams produced under systematically varied conditions of composition and pressure of the gas supplied to the nozzle. These measurements were made at a photon energy that is high enough to ionize all of the components; for convenience we used 584 Å (21.2 eV), the energy of the He I line. Our experience to date with several systems is that even with photon energies as large as 21 eV a weak

complex A·B produces mostly A⁺ ions (where A is the moiety of lower ionization potential.) Formation of high-threshold fragment ions of A from A·B is much less probable than the formation of A⁺. This phenomenon is useful because it means that the intensity of appropriate fragment ions of A provides a direct measure of the amount of uncomplexed A in the molecular beam. Thus, the ratio of intensities of A⁺ and a prominent fragment (A - n)⁺, viz. [A⁺]/[(A - n)⁺] depends on the content of A·B + A·A (+ higher clusters that give A⁺). This ratio is used to accomplish the needed optimization, as shown by example in the next section.

The production of A⁺ from the unavoidable A·A must be expected to interfere with the experiment. It can be minimized to some extent by expanding a gas mixture rich in B and poor in A to provide as large a ratio of A·B to A·A as feasible. Data to make the necessary correction are obtained by forming a beam containing A·A but no A·B by expansion of a mixture of A plus a rare gas R_g, preferably helium, to minimize the formation of mixed clusters with R_g, and carrying out a measurement of the photoefficiency function for the process A·A + hν → A⁺ + A + e analogously to the difference measurement already described for A·B. Additionally, it is necessary to measure the intensity ratios for dimer-originated A⁺ and some other ion that can come only from A·A, e.g., A₂⁺ itself, for both the A + R_g beam and the A + B beam. The fraction of the A⁺ produced from the A + B beam that stems from A·A is then simply the ratio

$$\text{fraction of A}^+ \text{ from A}\cdot\text{A} = \left(\frac{[\text{A}^+]}{[\text{A}\cdot\text{A}^+]}\right)_{\text{A}+\text{R}_g} / \left(\frac{[\text{A}^+]}{[\text{A}\cdot\text{A}^+]}\right)_{\text{A}+\text{B}} \quad (2)$$

provided that the ratios are measured at sufficiently low pressures that contributions, especially of A·A⁺, from trimers and heavier clusters are insignificant. For convenience, the intensities of A⁺ and A·A⁺ can be measured at different wavelengths as long as normalization to the circulating current of the electron storage ring is done. Mixed complexes in the A + R_g expansions could interfere with the above, but there is no evidence for such a difficulty in the cases reported here, most likely because the A·A bond strengths are substantially larger than the A·R_g bond strengths. This is consistent with the strikingly low nozzle pressures (~ 200 torr when R_g = Ar) at which useful intensities of A·A⁺ ions and fragment A⁺ ions are already observed.

Since the dimers are formed in an isentropic jet expansion, they are cooled below the temperature of the source gas. In this report the effective temperature of the beam T_B, including both monomers and dimers, is estimated using the following expression:

$$T_B = T_0 [1 + 4.8 \times 10^4 (\gamma - 1)^5 (P_0 \mathcal{D})^{2(\gamma-1)/\gamma}]^{-1} \quad (3)$$

where T₀ and P₀ are the temperature (K) and pressure (atm) of the source gas, \mathcal{D} is the nozzle diameter (cm), and $\gamma = C_p/C_v$ is the ratio of heat capacities of the source gas at constant pressure and at constant volume. This equation results from the adjustment of theoretical expressions^{15a,b} with an empirical calibration function designed to reproduce the known behavior of a similar nozzle beam system.^{15b,c} In the range 1.25 $\leq \gamma < 1.67$ it is expected to be accurate to $\pm 33\%$. For gas mixtures the practical value of γ is calculated from the rule

$$\gamma = 1 + \left\{ \sum F_i / (\gamma_i - 1) \right\}^{-1} \quad (4)$$

where F_i is the mole fraction of constituent i having value γ_i . Values of γ used here (or values of C_p, from which $\gamma = C_p/(C_p - R)$) are taken from ref 16a-c.

In the threshold technique described above for the measurement of D(A·B), excitation energy in the weak bond of the complex, together with the rotational energy, must be expected to be readily available for dissociation.¹⁷ The former could be a significant correction if the effective beam temperature is comparable to the bond strength. In this work the measured D_{T_B}(A·B) or P_{A,AB}(T_B) at beam temperature T_B is corrected to D₀(A·B) or P_{A,AB}(0) at 0 K, by addition of the vibrational excitation energy \mathcal{F}_{T_B} available for dissociation, plus the rotational energy.

$$\begin{aligned} D_0(\text{A}\cdot\text{B}) &= D_{T_B}(\text{A}\cdot\text{B}) + \mathcal{F}_{T_B} + \frac{3}{2}RT_B \\ P_{\text{A,AB}}(0) &= P_{\text{A,AB}}(T_B) + \mathcal{F}_{T_B} + \frac{3}{2}RT_B \end{aligned} \quad (5)$$

(15) (a) J. B. Anderson and J. B. Fenn, *Phys. Fluids*, **8**, 780 (1965); (b) R. E. Smalley, L. Wharton, and D. H. Levy, *J. Chem. Phys.*, **63**, 4977-4989 (1975); (c) R. E. Smalley, B. L. Ramakrishna, D. H. Levy, and L. Wharton, *Ibid.*, **61**, 4363-4364 (1974).

(16) (a) S. W. Benson, F. R. Cruickshank, D. M. Golden, G. R. Haugen, H. E. O'Neal, A. S. Rodgers, R. Shaw, and R. Walsh, *Chem. Rev.*, **69**, 279-324 (1969); (b) S. W. Benson, "Thermochemical Kinetics", Wiley, New York, 1976; (c) "International Critical Tables", Vol. 5, E. W. Washburn, Ed., McGraw-Hill, New York, 1929, p 80.

(17) P. M. Guyon and J. Berkowitz, *J. Chem. Phys.*, **54**, 1814-1826 (1971).

All of the complexes studied in this work are nonlinear with large moments of inertia, for which $3/2RT_B$ is an adequate approximation to the energy in rotation. To evaluate \mathcal{F}_{T_B} it is assumed, for simplicity, that all of the vibrational energy available for dissociation is contained in the new normal modes that are created upon complexation, and that the population probabilities of these modes simulate the equilibrium distribution at the beam temperature. Thus, assuming that the normal modes pertain to harmonic oscillators only,¹⁸

$$\mathcal{F}_T = \sum_i \frac{\epsilon_i}{\exp(\epsilon_i/kT) - 1} \quad (6)$$

where ϵ_i are the fundamental energies of the new normal modes and k is the Boltzmann constant. The summation includes at most six terms (for two nonlinear polyatomic moieties). Unfortunately, there is almost no information available on ϵ_i at present. Recently a set of all six ϵ_i was measured in Levy's laboratory for the T-shaped dimer of *s*-tetrazine.¹⁹ Because of the paucity of other reliable information, we have arbitrarily chosen to use these data for all complexes studied in this work, only adjusting for reduced mass and energy scale; i.e., we use

$$\epsilon_i = \xi_i [\tilde{\mu}/\mu]^{1/2} [D_0(A\cdot B)/\tilde{D}_0] \quad (7)$$

where μ is the reduced mass, and the diacritic indicates the data for *s*-tetrazine T dimers. We used 4.14 kcal/mol for \tilde{D}_0 , midway between Levy's reported upper and lower limits of 4.38 and 3.90 kcal/mol (a reasonable estimate is used for $D_0(A\cdot B)$ at first, and refined by iteration).

Results

Dissociation Energy for $t\text{-C}_4\text{H}_8\text{SO}_2 \rightarrow t\text{-C}_4\text{H}_8 + \text{SO}_2$. We wish to find a nozzle pressure and gas composition such that C_4H_8^+ ions from *trans*-2-butene- SO_2 can be observed with insignificant interference from trimers and larger clusters, and for which the correction for contributions from $(t\text{-C}_4\text{H}_8)_2$ is as small as practicable. Photoionization of a cluster-free nozzle beam of neat *t*- C_4H_8 at 584 Å shows that there is extensive fragmentation; about two-thirds of the ions produced are distributed among more than 10 different hydrocarbon ions containing two or three carbon atoms, and about one-third of the ions contain four carbon atoms. When mixtures of *t*- C_4H_8 and SO_2 are supplied to the nozzle and the resulting beams are examined at pressures up to 1000 torr, the relative intensities among the two- and three-carbon ions are unaffected, but the four-carbon ions show significant changes. In particular, the intensity of the hydrocarbon parent ion C_4H_8^+ grows very markedly with respect to the other ions as the pressure is raised. On the other hand, the relative amounts of the ions SO_2^+ and SO^+ show no effects that can be ascribed to the presence of *t*- C_4H_8 in the mixtures. These facts are consistent with the expected picture in which very little or no two-carbon and three-carbon ions are produced from clusters, and we therefore assume that they can be used to monitor the relative intensity of neutral monomer *t*- C_4H_8 in the molecular beam. Normalization to the intensities of the two- and three-carbon ions then allows the mass spectrum of the clusterless reference beam to be subtracted from the mass spectrum of a cluster-containing beam, to give the mass spectrum resulting from the photoionization of the clusters alone. For example, for the clusters present in the expansion at 800 torr of *t*- $\text{C}_4\text{H}_8 + \text{SO}_2$ in the ratio of 1:19, the relative intensities (%) of hydrocarbon-containing ions (ignoring tetramers and larger clusters) whose production probabilities exceed 1% are: C_4H_5^+ , 1.0; C_4H_6^+ , 1.4; C_4H_7^+ , 5.6; C_4H_8^+ , 60; $^{13}\text{C}_4\text{H}_8^+ + \text{C}_4\text{H}_9^+$, 3.0; $(\text{C}_4\text{H}_8)_2^+$, 4.4; $\text{C}_4\text{H}_8\text{SO}_2^+$, 5.4; $(\text{C}_4\text{H}_8)_2\text{SO}_2^+$, 6.3% and $\text{C}_4\text{H}_8(\text{SO}_2)_2^+$, 11.5, after correction for the efficiency of the mass spectrometer. The ancillary experiments gave <2% for the relative intensity of SO_2^+ produced from hydrocarbon-containing clusters. It is to be expected⁴ that the clusters produced in the jet expansion and found in the molecular beam as the nozzle pressure is increased from very low values will be dominated at first by the dimers, but with the trimers steadily increasing their share at the expense of the dimers as the pressure continues to rise. This pattern is verified by the data shown in Figure 2, which displays

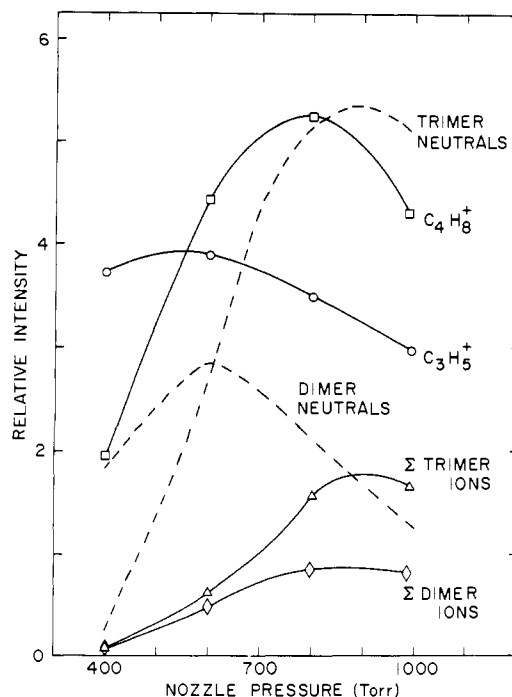


Figure 2. Points and solid lines: dependence of the intensities of various ions on nozzle pressure at 584 Å for the gas mixture *trans*-2-butene/ $\text{SO}_2 = 1:19$. "Σ trimer ions" means the sum of the intensities of $(\text{C}_4\text{H}_8)_3^+$, $(\text{C}_4\text{H}_8)_2\text{SO}_2^+$, and $\text{C}_4\text{H}_8(\text{SO}_2)_2^+$. "dimer ions" means the sum of the intensities of $(\text{C}_4\text{H}_8)_2^+$ and $\text{C}_4\text{H}_8\text{SO}_2^+$. The intensity of the ion C_4H_8^+ is that from the dissociative ionization of clusters only; the intensity of C_4H_8^+ from monomers *t*- C_4H_8 has been subtracted. The intensities of the ions with respect to each other have been corrected for quadrupole efficiency. Dashed lines: the dependence on nozzle pressure of the relative beam densities of neutral dimers *t*- $\text{C}_4\text{H}_8\text{SO}_2 + (t\text{-C}_4\text{H}_8)_2$ and neutral trimers $(t\text{-C}_4\text{H}_8)_3 + (t\text{-C}_4\text{H}_8)_2\text{SO}_2 + t\text{-C}_4\text{H}_8(\text{SO}_2)_2$, calculated from the ion intensities as described in ref 20.

the dependence on nozzle pressure of the observed intensities, corrected for mass spectrometer efficiency, of trimer, dimer, and fragment monomer ions. The trimer ion intensity is the sum of the intensities of $(\text{C}_4\text{H}_8)_3^+$, $(\text{C}_4\text{H}_8)_2\text{SO}_2^+$, and $\text{C}_4\text{H}_8(\text{SO}_2)_2^+$, the dimer ion intensity is the sum of the intensities of $(\text{C}_4\text{H}_8)_2^+$ and $\text{C}_4\text{H}_8\text{SO}_2^+$, and the plotted fragment monomer ion intensity is the intensity of C_4H_8^+ from the photoionization of clusters alone. As detailed in ref 20, the relative beam densities of the neutral dimers and trimers can be calculated from the observed ion intensity data, and are shown in Figure 2 as dashed lines (here, the analysis is in terms of the summed dimers and trimers, but that is a good approximation in this case). The beam density of neutral dimers maximizes at about 600 torr, at which pressure the density of neutral trimers is comparable. Note that this maximum occurs at a pressure substantially below that at the maximum of the dimer ion signal. Although the optimum nozzle pressure for dimers is 600 torr, it may be necessary to operate at a lower pressure to minimize possible interference from C_4H_8^+ ions produced from the trimers. To establish the extent of such interference at the neutral dimer maximum, preliminary threshold functions were measured at 500 and 800 torr, for which pressures the neutral trimer density rises by a factor 3.7, while the dimer density shows a slight net decrease. Unexpectedly, no evidence for the contribution of C_4H_8^+ intensity from trimers could be seen; the two threshold functions are identical in shape and onset within experimental error, and the intensity of the 800-torr function is slightly smaller than the intensity of the 500-torr function, in line with the slight net drop in neutral dimer beam density. An operating nozzle pressure of 600 torr was therefore selected for this case.

A number of reasons can be offered to account for the lack of intensity of C_4H_8^+ ions produced from trimers. (1) The reaction

(18) See, e.g., G. S. Rushbrooke, "Introduction to Statistical Mechanics", Oxford, London, 1949.

(19) L. Young, C. A. Haynam, and D. H. Levy, *J. Chem. Phys.*, **79**, 1592-1604 (1983).

(20) J. R. Grover and E. A. Walters, manuscript in preparation.

Table I. Ion Intensities^a for Photoionization at 584 Å of Molecular Beams Formed by Expansion of Various Mixtures of *trans*-2-Butene and SO₂ at a Nozzle Pressure of 600 torr at 23 °C

C ₄ H ₈ :SO ₂	C ₃ H ₅ ^{+b}	excess C ₄ H ₈ ^{+c}	(C ₄ H ₈) ₂ ⁺	(C ₄ H ₈ :SO ₂) ⁺
1:4	2.23	1.00	0.034	0.023
1:9	1.43	0.75	0.039	0.043
1:19	0.90	1.05	0.047	0.064

^a Corrected for quadrupole efficiency. All intensities are normalized to the intensity of excess C₄H₈⁺ for the 1:4 mixture. ^b Fragment ion produced only from uncomplexed *t*-C₄H₈ (with 37% probability). ^c Ion intensity only from dimers and larger clusters. The contribution of C₄H₈⁺ from uncomplexed *t*-C₄H₈ has been subtracted.

(*t*-C₄H₈)₃ + *hν* → C₈H₁₆ + C₄H₈⁺ + e would have a threshold of only about 8.8 eV (~1410 Å) if the C₈H₁₆ is the same as the product of the Woodward–Hoffman forbidden 2 + 2 concerted cycloaddition reaction. No trace could be found of an onset corresponding to this product (see Figures 3 and 4). If only van der Waals type bonds between pairs of molecules are involved, then it is reasonably estimated that the threshold for the reaction (*t*-C₄H₈)₃ + *hν* → (*t*-C₄H₈)₂ + C₄H₈⁺ + e could be several kcal mol⁻¹ higher than that for the dissociative ionization of the dimer. (2) Similarly, the reactions (*t*-C₄H₈)₂SO₂ + *hν* → C₄H₈SO₂ + C₄H₈⁺ + e and *t*-C₄H₈(SO₂)₂ + *hν* → S₂O₄ + C₄H₈⁺ + e would both be expected to have thresholds several kcal mol⁻¹ higher than that for the dimer because there are no strongly bound species corresponding to C₄H₈SO₂ or S₂O₄ that can reasonably be produced. (3) In general, it is not to be unexpected that the threshold for the production of monomer ions from van der Waals trimers will be higher than the corresponding threshold for dimers whenever two bonds must be broken in the trimer. The lack of monomer ions when an exothermic addition reaction could occur in the residual neutral dimer that would lower the trimer's threshold means that that reaction is too improbable to be detected. (4) The lifetime of a trimer ion at energies near its dissociation threshold will be very long compared with the corresponding dimer ion, because it has a much larger density of states due to the larger number of low-frequency normal modes associated with the van der Waals bonds. A long lifetime will give rise to a "kinetic effect"^{21,22} in which the apparent threshold occurs at a higher energy than the true threshold. Approximate calculations²¹ show that threshold increases in the range of 0.3 to 3 kcal mol⁻¹ are to be expected, the present case giving only ~0.2 kcal mol, however. (5) A possibly useful rule of thumb is to expect that often in the dissociative ionization of a trimer the charge will reside predominantly on the specie of lower ionization potential. Note, however, that this rule might not apply in this case, because the ionization potentials of both (SO₂)₂ (11.72 eV^{4d}) and *t*-C₄H₈:SO₂ (9.19 eV) are larger than that of *t*-C₄H₈ (9.13 eV) (see Figure 6).

There are three dimers in the *t*-C₄H₈ + SO₂ system, two of which, C₄H₈:SO₂ and (C₄H₈)₂, give rise to C₄H₈⁺ ions, and it is therefore desirable to minimize the contribution from (*t*-C₄H₈)₂. Table I gives the dependence on composition of the intensities of the ions (C₄H₈:SO₂)⁺ and (C₄H₈)₂⁺, and of the ion C₄H₈⁺ from C₄H₈:SO₂, (C₄H₈)₂ and larger clusters. The proportion of monomeric *t*-C₄H₈ in the beam decreases with increasing dilution of *t*-C₄H₈ by SO₂, as indicated by the decreasing intensity of the fragment ion C₃H₅⁺, which is a product only of the dissociative photoionization of monomeric *t*-C₄H₈. Surprisingly, the intensity of C₄H₈⁺ from dimers and clusters changes only modestly and the intensity of dimer ions increases. The ratio [(C₄H₈:SO₂)⁺]/[(C₄H₈)₂⁺] increases much less than expected and desired. This emphasizes the well-known fact that the nozzle expansion of gas mixtures is a highly complex dynamic system that is as yet poorly understood. However, further work to optimize the intensity of excess C₄H₈⁺ and the ratio [(C₄H₈:SO₂)⁺]/[(C₄H₈)₂⁺] was not required for this study, and the 1:19 gas mixture was therefore

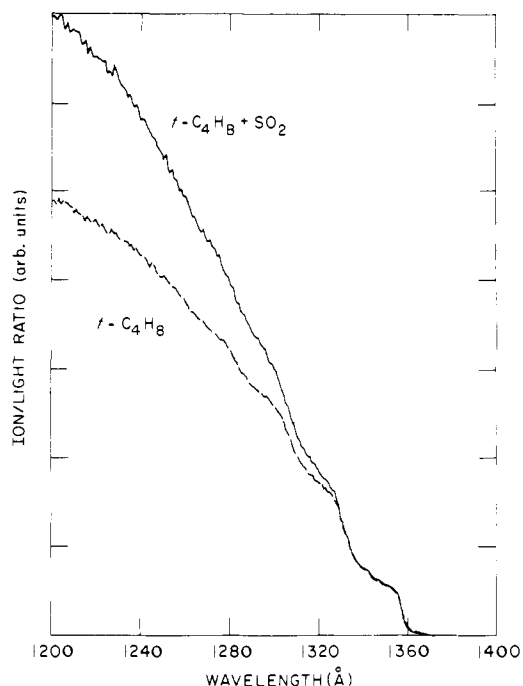


Figure 3. Photoionization efficiency for the production of C₄H₈⁺ from molecular beams. (a) Dashed line: beam from the nozzle expansion of neat *t*-C₄H₈ at 100 torr. (b) Solid line: beam from the nozzle expansion of a *t*-C₄H₈ + SO₂ mixture in the proportions 1:19 at 600 torr. The two curves are normalized to one another in the wavelength range 1343 to 1356 Å.

chosen for the measurement of *D*(*t*-C₄H₈:SO₂). As described further on, the contribution of C₄H₈⁺ from (*t*-C₄H₈)₂ in the threshold region was evaluated explicitly using eq 2 and found to be small. The relative insignificance of this correction may be rather general, a reason for which is given in the Discussion and evidence for which is accumulating as more cases are studied.

The photoionization efficiency function for the production of C₄H₈⁺ was measured at 1-Å intervals from 1200 to 1400 Å for the chosen conditions, viz. 600 torr nozzle pressure of premixed source gas in the proportions of 1.000 part of *trans*-2-butene (Matheson, CP) to 19.00 parts of sulfur dioxide (Linde, anhydrous), and measured again in the same spectral region at the same intervals for 100 torr nozzle pressure of neat *trans*-2-butene. The former measurement required 281 s per point, for a total of 16 h of beam time, distributed over nine fills of the storage ring, to achieve ion counts of 40 000 at 1250 Å, 32 000 at 1300 Å, and 8300 just above the threshold at 1350 Å. The 100-torr function was measured to a total ion count about twice as large in 185 s per point, 10 h of beam time, distributed over seven fills. The threshold step of both curves, taken for calibration to be 9.130 eV¹¹ (at the midpoint of the step rise¹⁷) is seen to be as sharp as the resolution of 3-Å fwhm permits. The latter data were normalized to the former in the range 1343 to 1356 Å, and both are plotted in Figure 3. The additional C₄H₈⁺ contributed from the complexes (and larger clusters) is clearly apparent and, below 1300 Å, substantial. The difference between the two data sets, calculated as described above, is shown in Figure 4, plotted as a function of photon energy. The error bars reflect the counting statistics. The approach to threshold is conspicuously linear, as also shown in the inset, which expands the threshold region. The long-dashed line shows the very small contribution of the homodimers (*t*-C₄H₈)₂. The sharpness of the threshold shows that the beam temperature is well below 23 °C, as can be seen by comparison with a calculated curve that depicts an assumed linear threshold function modified by thermal energy¹⁷ at 296 K, plotted as the short-dashed line. The low frequencies of the van der Waals modes render the threshold region especially susceptible to thermal blurring.

To evaluate the threshold energy and estimate its uncertainty, linear threshold functions were used. Calculations of chi-square

(21) L. Friedman, F. A. Long, and M. Wolfsberg, *J. Chem. Phys.*, **26**, 714 (1957).

(22) W. A. Chupka, *J. Chem. Phys.*, **30**, 191–211 (1959).

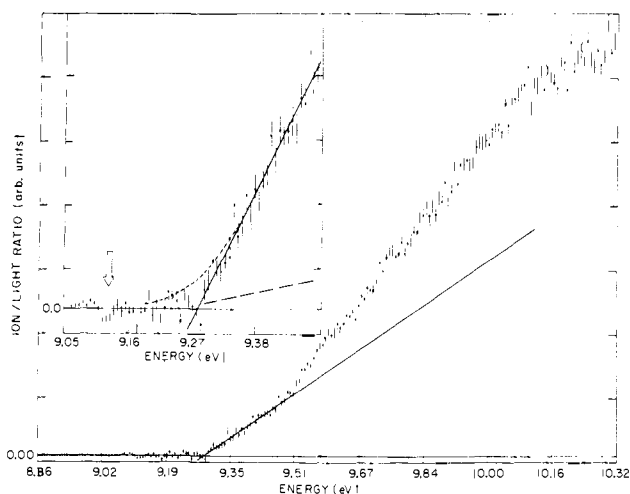


Figure 4. Production of $C_4H_8^+$ by dissociative photoionization of $t-C_4H_8 \cdot SO_2$, obtained as the difference of the normalized data shown in Figure 3. The inset shows the threshold region expanded. The straight lines are a least-squares fit to the data. The arrow in the inset marks the ionization potential of $t-C_4H_8$. The long-dashed line shows the contribution of $C_4H_8^+$ from $(t-C_4H_8)_2$ calculated according to eq 2 (see also Figure 7). The short-dashed line shows the deviation from linearity to be expected for a beam temperature of 296 K.

per degree of freedom, χ^2/η ,²³ show that a straight line is the simplest mathematical function needed to fit the data, and that more complicated functions only result in unacceptably low rejection levels and are therefore neither necessary nor supportable. A physical argument for approximately straight-line threshold functions can be made (see Discussion). This simple function provides an objective method of analysis consistent with the data that results in a threshold that should be close to the true one. Systematic variation of the slopes and thresholds of the assumed lines yielded a corresponding table of χ^2/η . The slope and threshold for which χ^2/η has its minimum value give the best fit. The maximum possible number of experimental points above the threshold was used in the analysis, with the constraint that the minimum $\chi^2/\eta \lesssim 1.05$. To estimate the experimental uncertainty, the calculated table was used to find the highest and lowest threshold values consistent with the published values²⁴ of χ^2/η corresponding to the 95% confidence level. From these values highest and lowest thresholds encompassing a 68% confidence level were calculated in order to quote an uncertainty comparable to one standard deviation. This uncertainty must then be convoluted with that arising from the uncertainty in the position of the zero line (see Figure 4). The resulting threshold value is 9.280 ± 0.008 eV. Correction for the very small contribution from $(t-C_4H_8)_2$ increases this value slightly, to $P_{A,AB} = 9.284 \pm 0.008$ eV, which corresponds to a dissociation energy of $D(t-C_4H_8 \cdot SO_2) = 3.54 \pm 0.18$ kcal/mol at the temperature of the molecular beam. The latter may be estimated from eq 3 to be 40 ± 13 K, where $\gamma = 1.265$ for SO_2 ^{16b} and 1.104 for $t-C_4H_8$.^{16a} Equation 5 then gives, for this beam temperature, an additive energy correction of $\mathcal{F}_{T_B} + \frac{3}{2}RT_B = 0.31 \pm 0.15$ kcal/mol, yielding, finally, $D_0(t-C_4H_8 \cdot SO_2) = 3.85 \pm 0.23$ kcal/mol, and a similarly corrected threshold at 0 K of $P_{A,AB}(0) = 9.297 \pm 0.010$ eV.

The reference molecular beam resulting from a nozzle pressure of 100 torr of neat *trans*-2-butene has a higher calculated temperature than above, $T_B \approx 250$ K. However, the monomer parent ion in each spectrum displays clear step-like behavior at the ionization threshold (Figure 3) limited only by the optical resolution, so that domination by the adiabatic transition is reasonably certain.¹¹ Hot band effects cannot be excluded (see Figure 4) but are very small and cannot at present be proven because of comparable small effects due to instability in the size and position

(23) See, e.g., W. C. Hamilton, "Statistics in Physical Science", Ronald Press: New York, 1964.

(24) A. Hald in "Handbook of Tables for Probability and Statistics", W. H. Beyer, Ed., Chemical Rubber Co., Cleveland, 1966, pp 235–238.

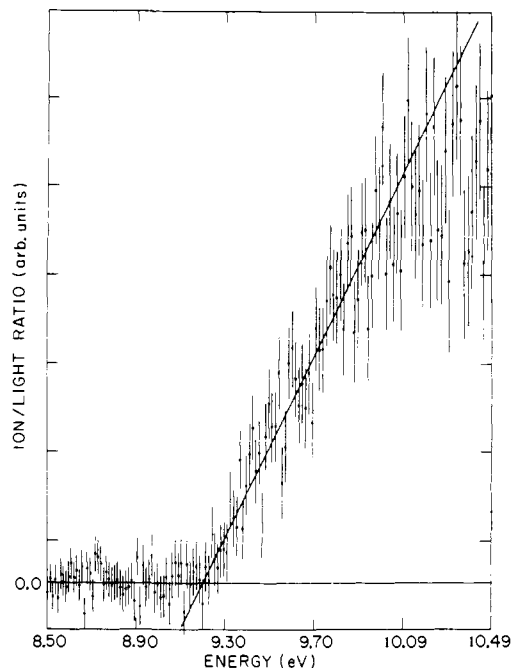


Figure 5. Threshold region of photoionization of $t-C_4H_8 \cdot SO_2$ to produce $(C_4H_8 \cdot SO_2)^+$. The solid line is the least-squares straight line fit to the first 54 points above the threshold.

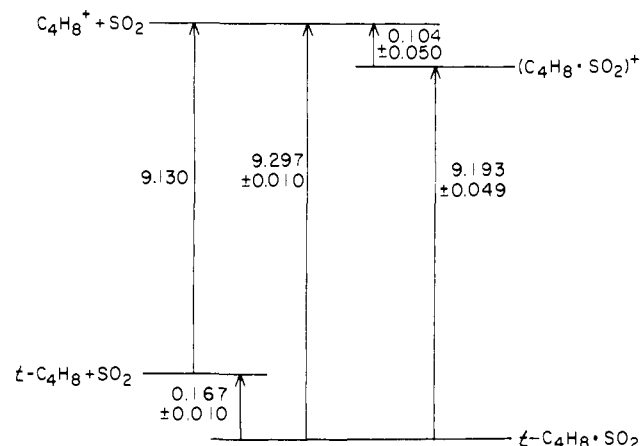


Figure 6. Summary of energy relationships of *trans*-2-butene/sulfur dioxide neutral and ionic complexes (not drawn to scale). All energies are in electron volts.

of the electron beam photon source, which instability causes systematic deviations from the zero line just below I_A (arrow). As the storage ring operations improve, the electron beam will be stabilized and this type of effect will diminish. We therefore believe there is negligible error resulting from the wavelength normalization of the two spectra to each other (± 0.001 eV).

Dissociation Energy for $(C_4H_8 \cdot SO_2)^+ \rightarrow C_4H_8^+ + SO_2$. The threshold region for photoionization of $t-C_4H_8 \cdot SO_2$ to produce $(C_4H_8 \cdot SO_2)^+$ was measured. At the precision of this experiment (Figure 5) the resulting ionization potential is $I_{AB} = 9.193 \pm 0.049$ eV. This value is quite interesting because it can be used to calculate the dissociation energy of the parent ion of the complex, viz. $(C_4H_8 \cdot SO_2)^+ \rightarrow C_4H_8^+ + SO_2$, via the relation $D_0[(C_4H_8 \cdot SO_2)^+] = P_{A,AB}(0) - I_{AB}$, giving the result 2.4 ± 1.2 kcal/mol. This energy is significantly smaller than the values of ≥ 10 kcal/mol nearly always observed and expected²⁵ for the ion-neutral binding of polyatomic molecules. Surprisingly, it is even smaller than the neutral-neutral binding of $t-C_4H_8$ to SO_2 .

The results of this work for the *trans*-2-butene/sulfur dioxide complex are summarized in Figure 6.

(25) C. Y. Ng, *Adv. Chem. Phys.*, **52**, 263–362 (1983).

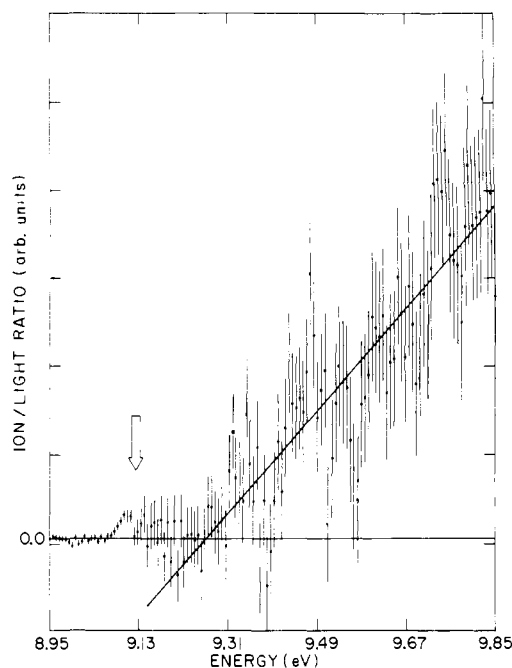


Figure 7. Threshold region of dissociative photoionization of $(t\text{-C}_4\text{H}_8)_2$ to produce C_4H_8^+ . The solid line is the least-squares straight line fit to the first 74 points above the threshold. The arrow marks the ionization energy of $t\text{-C}_4\text{H}_8$.

Dissociation Energy for $(t\text{-C}_4\text{H}_8)_2 \rightarrow \text{C}_4\text{H}_8 + \text{C}_4\text{H}_8$. Using the beam formed from the mixture $t\text{-C}_4\text{H}_8$ and Ar in the proportions 1:4, an efficiency spectrum was measured for the production of C_4H_8^+ at wavelengths from 1200 to 1400 Å at 1-Å intervals. Total ion counts accumulated were very substantial, comparable to the 100-torr spectrum of neat $t\text{-C}_4\text{H}_8$ already described. The same type of analysis was carried out and the resulting difference spectrum is shown in Figure 7. The results are of markedly lower quality than those for $t\text{-C}_4\text{H}_8\cdot\text{SO}_2$ despite the significantly larger amount of ion counts accumulated; contrast Figure 7 with Figure 4. Application of the χ^2/η minimization procedure to these data, assuming a straight-line threshold function, yields a threshold value of 9.250 ± 0.049 eV at a calculated beam temperature of 18 ± 6 K, which, corrected to 0 K, gives $P_{A,AA}(0) = 9.254 \pm 0.049$ eV. This corresponds to a dissociation energy $D_0[(t\text{-C}_4\text{H}_8)_2] = 2.9 \pm 1.1$ kcal/mol. The weakness of the signal plus the similarity of this threshold to that of C_4H_8^+ from $t\text{-C}_4\text{H}_8\cdot\text{SO}_2$, i.e., $P_{A,AB} \approx P_{A,AA}$, are the reasons that the contribution of C_4H_8^+ from the homodimer $(t\text{-C}_4\text{H}_8)_2$ is not a serious problem in the measurement of $D_0(t\text{-C}_4\text{H}_7\cdot\text{SO}_2)$, as shown by the long-dashed line in Figure 4.

Dissociation Energy for $\text{C}_6\text{H}_6\cdot\text{SO}_2 \rightarrow \text{C}_6\text{H}_6 + \text{SO}_2$. The two gas mixtures for jet expansion were sulfur dioxide and argon saturated with benzene vapor at 23 °C at a total bubbler head pressure of 800 torr. The ion $\text{C}_6\text{H}_6\cdot\text{SO}_2^+$ is produced only very weakly so the complex $\text{C}_6\text{H}_6\cdot\text{SO}_2$ must fragment essentially completely upon photoionization. Spectra for the production of C_6H_6^+ were measured in the wavelength range 1180 to 1380 Å at 1-Å intervals, both for $\text{C}_6\text{H}_6 + \text{SO}_2$, at 600-torr nozzle pressure, and for $\text{C}_6\text{H}_6 + \text{Ar}$ at 100 torr where the beam's content of the homodimers $(\text{C}_6\text{H}_6)_2$ is very small.²⁰ The difference spectrum, shown in Figure 8, displays a remarkably clean straight-line approach to the threshold at 9.422 ± 0.009 eV, where for calibration the benzene photoionization threshold was taken to be $I_A = 9.248$ eV.¹¹ The dissociation energy is then $D(\text{C}_6\text{H}_6\cdot\text{SO}_2) = 4.00 \pm 0.20$ kcal/mol at a calculated beam temperature of 48 ± 16 K ($\gamma = 1.113^{16a}$ for benzene). Correction for the beam temperature according to eq 5 gives $D_0(\text{C}_6\text{H}_6\cdot\text{SO}_2) = 4.40 \pm 0.28$ kcal/mol and $P_{A,AB}(0) = 9.439 \pm 0.012$ eV. No correction for the contribution of $(\text{C}_6\text{H}_6)_2$ is necessary, as shown in the next section.

Dissociation Energy for $(\text{C}_6\text{H}_6)_2 \rightarrow 2\text{C}_6\text{H}_6$. Using argon saturated with benzene²⁶ at a total pressure in the bubbler of 800

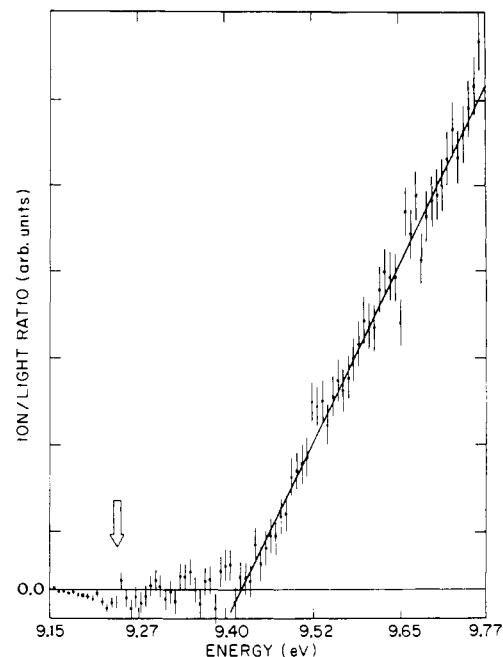


Figure 8. Threshold region of dissociative photoionization of $\text{C}_6\text{H}_6\cdot\text{SO}_2$ to produce C_6H_6^+ . The solid line is the least-squares straight line fit to the first 46 points above the threshold. The arrow marks the ionization potential of benzene.

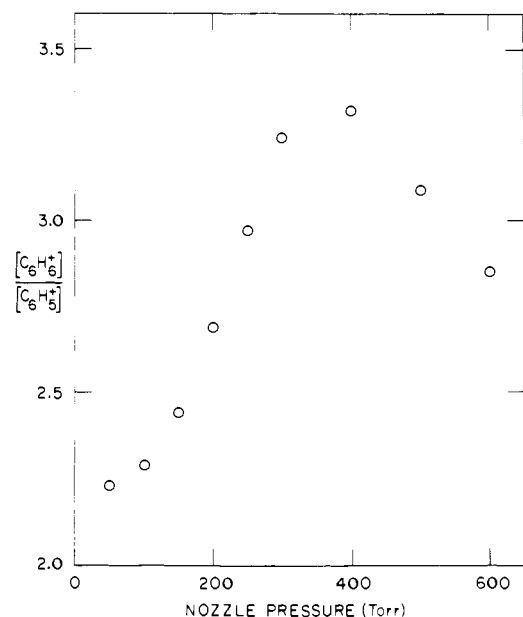


Figure 9. Dependence of the ratio $[\text{C}_6\text{H}_6^+]/[\text{C}_6\text{H}_5^+]$ on nozzle pressure for argon saturated with benzene at 800 torr and 23 °C. Photoionization carried out at 584 Å.

torr, the production of C_6H_6^+ from the dissociative photoionization of $(\text{C}_6\text{H}_6)_n$ at 584 Å is clearly seen. Figure 9 shows that the ratio $[\text{C}_6\text{H}_6^+]/[\text{C}_6\text{H}_5^+]$ maximizes near a nozzle pressure of 320 torr. The falloff to higher pressures suggests that the production of C_6H_6^+ from trimers and larger clusters is inefficient. Careful measurements were made of the production of C_6H_6^+ in molecular beams rich in $(\text{C}_6\text{H}_6)_2$, at a nozzle pressure of 266 torr,²⁰ in the wavelength range 1180 to 1380 Å at 1-Å intervals. Subtraction of the normalized dimer-poor beam formed at 100-torr nozzle pressure gave the result in Figure 10. There is no evidence for any production of C_6H_6^+ from benzene dimer at photon energies below 10 eV, although Figure 9 shows that it is produced in

(26) K. C. Janda, J. C. Hemminger, J. S. Winn, S. E. Novick, S. J. Harris, and W. Klemperer, *J. Chem. Phys.*, **63**, 1419-1421 (1975).

Table II. Collected Results of This Work^a

complex	D_T	T_B	D_0	D_0 [lit.]
$t\text{-C}_4\text{H}_8\cdot\text{SO}_2$	3.54 ± 0.18	40 ± 13	3.85 ± 0.23	3.79 ± 0.17^b
$(\text{C}_4\text{H}_8\cdot\text{SO}_2)^+$	2.1 ± 1.1	40 ± 13	2.4 ± 1.2	
$(t\text{-C}_4\text{H}_8)_2$	2.8 ± 1.1	18 ± 6	2.9 ± 1.1	
$\text{C}_6\text{H}_6\cdot\text{SO}_2$	4.00 ± 0.20	48 ± 16	4.40 ± 0.28	
$(\text{C}_6\text{H}_6)_2$		present technique appears unsuccessful		

^a D_T gives the measured dissociation energy of A·B at the beam temperature T_B , and D_0 is the dissociation energy at 0 K, calculated from D_T using eq 5. The beam temperature is calculated using eq 3. D_T and D_0 are in kcal/mol, and T_B is in kelvins. ^bCalculated from $\Delta E_{298} = 2.52 \pm 0.07$ reported in ref 27, using the relation $D_0 \approx \Delta E_T - 3RT + \mathcal{F}_T$ where $T = 298$ K. The indicated uncertainty reflects an assumed large uncertainty in the fundamental frequencies of the van der Waals normal modes (see text).

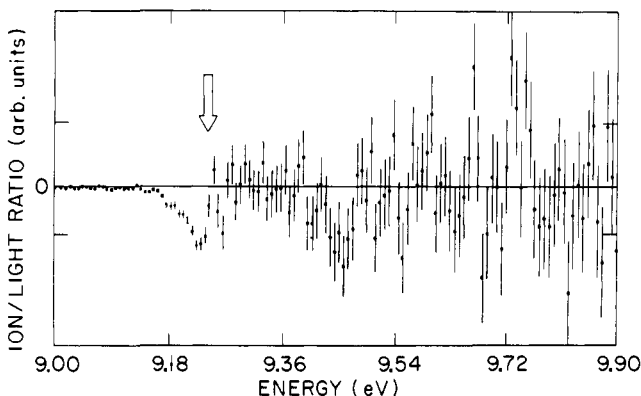


Figure 10. Difference plot attempt to observe dissociative photoionization of $(\text{C}_6\text{H}_6)_2$ to produce C_6H_6^+ . The arrow marks the ionization potential of benzene.

abundance at 21 eV (584 Å). Consequently the dissociation energy for $(\text{C}_6\text{H}_6)_2$ apparently cannot be measured by the subtractive technique described in this paper. On the other hand, there is no correction necessary for the contribution of C_6H_6^+ from $(\text{C}_6\text{H}_6)_2$ in the measurement of $D_0(\text{C}_6\text{H}_6\cdot\text{SO}_2)$ described in the preceding subsection.

The results of this work are collected in Table II.

Discussion

$t\text{-C}_4\text{H}_8\cdot\text{SO}_2$. Hanazaki²⁷ measured the thermodynamic energy of dissociation (constant volume) of the *trans*-2-butene/sulfur dioxide complex in the gas phase using spectrophotometric analysis of equilibrium mixtures of the two components. He obtained $\Delta E_{298}(t\text{-C}_4\text{H}_8\cdot\text{SO}_2) = 2.52 \pm 0.07$ kcal/mol. If it is assumed that the vibrational frequencies of the two components are essentially unchanged in the complexation, then the dissociation energy at 0 K can be estimated from Hanazaki's value by addition of \mathcal{F}_{298} , and subtraction of $3/2RT$ for translational and $3/2RT$ for rotational motion. For the calculation of \mathcal{F}_{298} the fundamental frequency values of the normal modes reported for the *s*-tetrazine dimer¹⁹ scaled according to eq 7 were used. To provide an idea of the uncertainty associated with their use, they were arbitrarily scaled up and down by a factor of $\sqrt{2}$, and corresponding values of \mathcal{F}_{298} were calculated. The result is $D_0(t\text{-C}_4\text{H}_8\cdot\text{SO}_2) = 3.79 \pm 0.17$ kcal/mol, in good agreement with the value 3.85 ± 0.23 kcal/mol obtained in the work reported here. Alternatively, using the expression

$$\mathcal{F}_T = D_0(\text{A}\cdot\text{B}) - \Delta E_T(\text{A}\cdot\text{B}) + 3RT \quad (8)$$

Hanazaki's value of ΔE_{298} combined with ours of D_0 yields $\mathcal{F}_{298} = 3.11 \pm 0.24$ kcal/mol, from which an effective fundamental mode frequency of $\epsilon = 54 \pm 30$ cm^{-1} can be calculated from eq 6, assuming that all six frequencies are the same. This value is quite reasonable for van der Waals modes. The wide limits of error show that even only rough approximations to the ϵ_i suffice to calculate reasonably accurate values of \mathcal{F}_T in this case. The comparison of Hanazaki's measurement with ours is important because it confirms a result of the gas-phase spectrophotometric equilibrium technique by a completely independent method.

The good agreement with the equilibrium work also suggests that our data pertain to the most strongly bound conformer, if more than one structure for $t\text{-C}_4\text{H}_8\cdot\text{SO}_2$ is possible. Two different structures have been observed, for example, for the *s*-tetrazine homodimers formed in jet expansions.²⁸ More weakly bound configurations of $t\text{-C}_4\text{H}_8\cdot\text{SO}_2$ either are not present, or if they are present, do not undergo dissociative photoionization to form C_4H_8^+ to a sufficient extent to be detected. In general, the effective presence of structural isomers will cause the apparent value of $D_0(\text{A}\cdot\text{B})$ measured by the threshold technique described here to be smaller than the value measured by an equilibrium method, because the observed threshold will always be that of the most weakly bound conformer. The good agreement also eliminates the possibility that only excited A^+ or B is produced, because this would result in a threshold that is too high.

Away from threshold one expects the shape of the photoefficiency spectrum for the production of A^+ from $\text{A}\cdot\text{B}$ to reflect several circumstances, each of which has its own onset or distinctive signature: (1) product excited states of either A^+ or B ; (2) isomers of $\text{A}\cdot\text{B}$ in the target beam; (3) contamination of the target beam with $\text{A}\cdot\text{A}$; (4) contamination of the target beam with trimers or larger clusters; (5) fragmentation of A^+ ; (6) residual autoionizing discrete states. In Figure 4 one sees an obvious onset at about 9.50 eV or somewhat below (depending on the shape of the threshold line). As already discussed, this structure is unlikely to be due to circumstances 2, 3, or 4, and it does not have the expected signature for 5 or 6. It is most likely, therefore, to be due to (1). However, our data provide no way to tell whether the excited state involved is in *trans*-2-butene ion or sulfur dioxide. The difference between threshold and onset is ~ 0.2 eV or ~ 1600 cm^{-1} . The nearest fundamental ground-state vibrational frequency of neutral sulfur dioxide is the asymmetric stretch²⁹ at 1362 cm^{-1} . The two combination lines nearest this energy are at $3\nu_2 = 1553$ cm^{-1} and $\nu_1 + \nu_2 = 1669$ cm^{-1} . In C_4H_8^+ ion, the first band in the photoelectron spectrum of *trans*-2-butene, taken with He I radiation (21.22 eV),³⁰ can be resolved into a progression showing four detectable maxima with a mean spacing of ~ 0.17 eV (~ 1400 cm^{-1}), the second member of which is the most intense. This same splitting gives rise to the pronounced stepwise structure of the curves in Figure 3. Now the first photoelectron band arises from the ejection of a bonding π -electron, so the observed progression is expected to be due mainly to the C=C stretch. We are not aware of any fundamental vibrational frequency assignments for C_4H_8^+ , but in neutral $t\text{-C}_4\text{H}_8$ this mode occurs at^{31,32} $\nu_4 = 1682$ cm^{-1} in the gas phase, reasonably near the observed line spacing. Our best judgment is that the onset near 9.5 eV is due to the production of C_4H_8^+ and SO_2 in vibrationally excited states, most likely with predominance of the first ($\nu = 1$) excited state of the

(27) I. Hanazaki, *J. phys. Chem.*, **76**, 1982–1989 (1972).

(28) C. A. Haynam, D. V. Brumbaugh, and D. H. Levy, *J. Chem. Phys.*, **79**, 1581–1591 (1983).

(29) G. Herzberg, "Molecular Spectra and Molecular Structure III", Van Nostrand, New York, 1966.

(30) R. M. White, T. A. Carlson, and D. P. Spears, *J. Electron Spectrosc. Relat. Phenom.*, **3**, 59–70 (1974); K. Kimura, S. Katsumata, Y. Achiba, T. Yamazaki, and S. Iwata, "Handbook of HeI Photoelectron Spectra of Fundamental Organic Molecules", Halsted Press, New York, 1981.

(31) J. E. Kilpatrick and K. S. Pitzer, *J. Res. Natl. Bur. Stand.*, **38**, 191–209 (1947).

(32) I. W. Levin, R. A. R. Pearce, and W. C. Harris, *J. Chem. Phys.*, **59**, 3048–3061 (1973).

C=C stretch and the $\nu = 1$ state of the asymmetric stretch of SO_2 .

This experiment by itself provides no information about the structure of the $t\text{-C}_4\text{H}_8\cdot\text{SO}_2$ complex. It is interesting in this connection that the heat of formation of the hypothetical valence compound *trans*-2,3-dimethylthiirane 1,1-dioxide at 300 K (as calculated using Benson's tables^{16b}) gives an energy for dissociation back into *t*-2-butene and SO_2 of about 4 kcal mol^{-1} , close to our observed dissociation energy. In addition to thermochemical information, structural information would be useful in understanding the well-known copolymerization of olefins with sulfur dioxide to form polysulfones,³³ for which reaction there is much evidence of the participation of 1:1 molecular complexes.^{33-36a} For *trans*-2-butene the heat of the copolymerization reaction (per unit) in the liquid phase of mixed reactants at 20°C is $\Delta H = -20.1 \text{ kcal/mol}$,³⁴ so the complex $t\text{-C}_4\text{H}_8\cdot\text{SO}_2$ is not the lowest state of the system. There is considerable practical interest in polysulfone resins,^{33b,c} recent concerns being their application as electron beam resists,³⁷ and as a means to substitute pollutant sulfur dioxide for expensive olefin in useful synthetic materials.^{36b}

$\text{C}_6\text{H}_6\cdot\text{SO}_2$. There is apparently no other measurement of the dissociation energy of the gas-phase benzene/sulfur dioxide complex to which comparison can be made with our result. Equilibrium constants have been measured for 1:1 complexes of benzene and sulfur dioxide in carbon tetrachloride³⁸ and *n*-hexane³⁹ solvents, the latter measurement giving $\Delta H = 1.03 \pm 0.15 \text{ kcal/mol}$ for the enthalpy of dissociation at 298 K. However, it is well known that dissociation energies of weak complexes are nearly always substantially different in the liquid than in the gas phase owing to dominating solvation effects.⁴⁰ There is also convincing qualitative evidence that the binding energy between benzene and sulfur dioxide is appreciable. Sulfur dioxide displays an order of magnitude higher room-temperature solubility in liquid benzene and other aromatic hydrocarbons than in saturated hydrocarbons.⁴¹ Also, solid 1:1, 1:2, and 1:3 complexes between alkylbenzenes and sulfur dioxide, stable at reduced temperatures, have been isolated.⁴²

It is noteworthy that the difference spectrum of the C_6H_6^+ ion (Figure 8) betrays the presence of the complex $\text{C}_6\text{H}_6\cdot\text{SO}_2$ in a conspicuous and convincing manner, while the parent ion ($\text{C}_6\text{H}_6\text{SO}_2$)⁺ can hardly be seen. As already discussed above, there is effectively no contribution by $(\text{C}_6\text{H}_6)_2$ or larger clusters $(\text{C}_6\text{H}_6)_n$ below 10 eV. Therefore, the data in Figure 8 constitute the indirect but unambiguous observation of the species $\text{C}_6\text{H}_6\cdot\text{SO}_2$ in the gas phase. It may be anticipated that such difference spectra will sometimes be a useful way to detect the presence of neutral dimers in a molecular beam when the parent complex ion cannot be seen at all.

Perhaps the most unexpected result of this work is the tendency for the fragmentation appearance potential threshold processes

(33) (a) D. S. Frederick, H. D. Cogan, and C. S. Marvel, *J. Am. Chem. Soc.*, **56**, 1815-1819 (1934); (b) R. D. Snow and F. E. Frey, *Ind. Eng. Chem.*, **30**, 176-182 (1938); (c) For a review, see N. Tokura in "Encyclopedia of Polymer Science and Technology", Vol. 9, Wiley, New York, 1968, pp 460-485.

(34) G. M. Bristow and F. S. Dainton, *Proc. R. Soc. London, Ser. A*, **229**, 509-524 (1955).

(35) W. G. Barb, *Proc. R. Soc. London, Ser. A*, **212**, 66-80 (1952).

(36) (a) P. Colombo, J. Fontana, and M. Steinberg, *J. Polym. Sci., Polym. Chem. Ed.*, **6**, 3201-3215 (1968); (b) M. Steinberg, *Polym. Eng. Sci.*, **17**, 335-339 (1977).

(37) E. Gipstein, W. Moreau, G. Chiu, and O. U. Need, III, *J. Appl. Polym. Sci.*, **21**, 677-688 (1977).

(38) L. J. Andrews and R. M. Keefer, *J. Am. Chem. Soc.*, **73**, 4169-4172 (1951); P. A. D. de Maine, *J. Chem. Phys.*, **26**, 1036-1041 (1957).

(39) D. Booth, F. S. Dainton, and K. J. Ivin, *Trans. Faraday Soc.*, **55**, 1293-1309 (1959).

(40) (a) R. S. Mulliken and W. B. Person, "Molecular Complexes", Wiley-Interscience, New York, 1969; (b) M. Kroll, *J. Am. Chem. Soc.*, **90**, 1097-1105 (1968).

(41) S. J. Lloyd, *J. Phys. Chem.*, **22**, 300-303 (1918); J. Horiuchi, *Bull. Inst. Phys. Chem. Res., Tokyo*, **9**, 697-703 (1930); H. Sano, *Nippon Kagaku Zasshi*, **89**, 362-368 (1968); W. Gerrard, *J. Appl. Chem. Biotechnol.*, **22**, 623-650 (1972); D. L. Costa and D. Underhill, *J. Am. Ind. Hyg. Assoc.*, **37**, 46-51 (1976).

(42) C. Mazzetti and F. de Carli, *Gazz. Chim. Ital.*, **56**, 34-36 (1926).

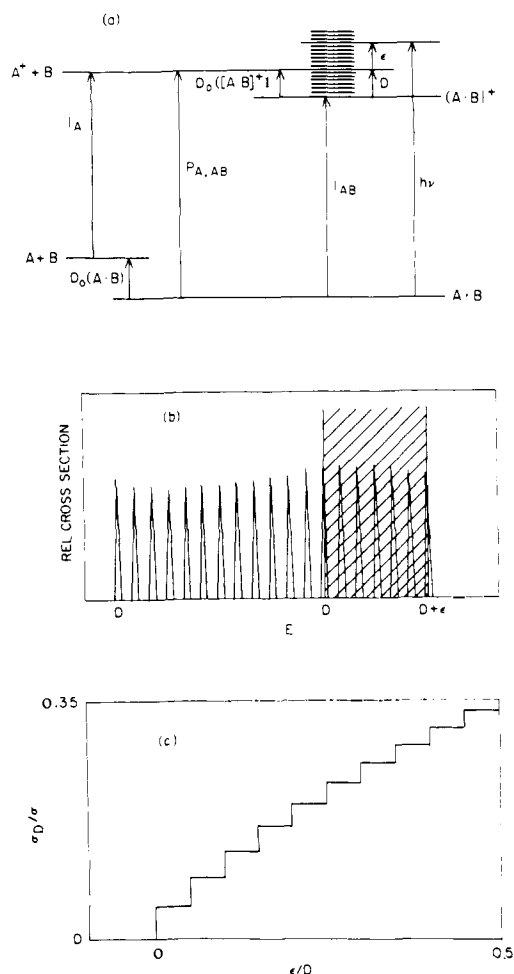


Figure 11. (a) Diagram illustrating relationship of energy symbols used in eq 9. (b) Schematic photoelectron spectrum of $A\cdot B^+$ as a function of excitation energy E in the product ion $(A\cdot B)^+$. (c) Threshold photoionization efficiency function for the production of A^+ from $A\cdot B$.

of the type $A\cdot B + h\nu \rightarrow A^+ + B + e^-$ to display such remarkable straight-line behavior. In addition to the examples already given in Figures 4 and 8, work in progress shows such behavior for several other cases as well. It is evidently a rather general phenomenon.

A straight-line threshold function can easily be rationalized in the following simplified picture. It is assumed that the molecule representing the moiety of lower ionization potential displays, as monomer, a photoionization efficiency function that begins with an abrupt step at threshold and is flat at cross section σ for some energy region above threshold. The corresponding photoelectron spectrum that gives rise to such a step consists of a single line. It is further assumed that when the photon interacts with the complex it excites mainly either one or the other moiety, and that Rydberg excitation leads to dissociation rather than autoionization, so that the observed ions arise from the direct ionization process.⁴³ The vibrationless level of the neat ion becomes, in the field of a weakly bound partner molecule, a band comprised of the new vibrational manifold of closely spaced levels created when the complex is formed. The photoelectron single line of the monomer then becomes split into a broad region of closely spaced lines. It is assumed that the Franck-Condon population envelope $f(E)$ of this band is flat, i.e., $f(E) \approx \text{constant}$, in the neighborhood of the threshold. If the ionic complex is also weakly bound, then above its dissociation energy, energy quickly transfers from the populated band levels into the dissociative mode. The cross section σ_D for this process, $A\cdot B + h\nu \rightarrow A^+ + B + e^-$, is then

(43) J. Berkowitz, "Photoabsorption, Photoionization and Photoelectron Spectroscopy", Academic Press, New York, 1979, p 129.

$$\sigma_D = \sigma \int_D^{D+\epsilon} f(E) dE / \int_0^{D+\epsilon} f(E) dE \quad (9)$$

$$\sigma_D = \sigma \epsilon / (D + \epsilon)$$

that is, $\sigma_D \propto \epsilon$ as long as $\epsilon \ll D + \epsilon$. Here, $D = D_0([A \cdot B]^+)$ is the dissociation energy of the ion, i.e., of the process $(A \cdot B)^+ \rightarrow A^+ + B$, and the ionic excitation energy in excess of the ion's dissociation threshold is ϵ . The relationship of the various energies is illustrated in Figure 11a. An idealized photoelectron spectrum of $A \cdot B$, expressed as a function of excitation energy E of the ion $(A \cdot B)^+$, is sketched in Figure 11b, where the hatched zone indicates the states that dissociate to form $A^+ + B$, and the corresponding threshold cross section is shown schematically in Figure 11c. The small steps are not resolved in practical experiments so the threshold cross section function appears smooth and nearly straight. Thus, in this simple picture the complexation causes a single, step-shaped photoionization efficiency function for the production of A^+ from A to become, at threshold, a straight line of slope σ/D that intercepts the abscissa just at the threshold $P_{A,AB}$. When $\epsilon \gg D$, σ_D approaches σ asymptotically. However, the latter behavior is usually hidden because a vibrationally excited state of the ion A^+ or its neutral partner B causes an overriding contribution of a new approximately linearly rising cross section (e.g., see Figure 3) similar to that already described for the ground state of A^+ . Note that if σ is not a step function, but rises more gradually from the ionization potential, then such straight-line threshold behavior for σ_D is not to be expected. We have observed that such is the case for the (allyl bromide)₂ and (allyl bromide-hydrogen chloride) complexes. Also, note that the slope of the threshold line is inversely proportional to D . This means that if the dissociation energy of the ionic complex is large, then the threshold line will be suppressed, most of the direct photoionization cross section going to form the dimer ion. This is entirely consistent with our observations; for $(C_4H_8 \cdot SO_2)^+$, for which D is only 2.4 kcal/mol, the threshold line is strong, but for $(C_6H_6)_2^+$, for which D is much larger, ~ 17.0 kcal/mol,⁴⁴ no threshold signal at all could be detected, although $C_6H_6^+$ ion from $(C_6H_6)_n$ is seen in abundance at 584 Å (see Figure 9).

As the excitation energy in a polyatomic ion decreases toward the minimum necessary for dissociation, the ion's lifetime becomes comparable to its dwell time in the ion extraction region of the instrument, and thereby causes the observed threshold to be larger than the true threshold^{21,22} (the "kinetic effect"). This effect should not be important for the work reported here because the ionic heterodimers are only weakly bound (vide infra). Near threshold the excitation energy of such a weakly bound ion is comparable to the fundamental frequency of only one or two normal modes of the isolated partners, and must therefore reside essentially entirely in the six (or fewer) soft modes of the weak bond to be broken. The level density of the complex system cannot then be large enough to delay the dissociation by the required amount of time ($> 10^{-5}$ s); reasonable calculations²¹ show that a downward correction to the observed threshold in the neighborhood of only about $-0.01 D_0([A \cdot B]^+)$ is to be expected.

The threshold cross sections for the production of A^+ by dissociative photoionization of weak complexes are much larger for heterodimers $A \cdot B$ than for homodimers $A \cdot A$ which circumstance is reflected in the uncertainty estimates in Table II. This is borne out for other cases as well. In the light of the foregoing discussion, it would appear that the dissociation energy generally tends to be larger for homodimer than for heterodimer ions. In fact this phenomenon has been studied previously.⁴⁴⁻⁴⁶ Illustrative examples are $D([CS_2 \cdot OCS]_2^+) = 5.8$ kcal/mol,^{47a} while $D([CS_2]_2^+)$

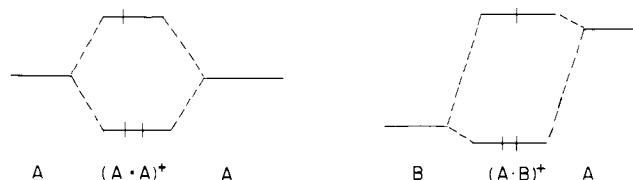


Figure 12. Comparison of the interactions of the highest occupied molecular orbitals of the partner molecules in the ions $(A \cdot A)^+$ and $(A \cdot B)^+$.

$= 17.5$ kcal/mol^{47b} and $D([OCS]_2^+) = 17.2$ kcal/mol^{47a}; $\Delta H([C_6H_6 \cdot CS_2]^+) = 12.2$ kcal/mol,^{45b} while $\Delta H([C_6H_6]_2^+) = 17.0$ kcal/mol,^{45b} and $D_0([C_6H_6 \cdot HCl]^+) = 7.3$ kcal/mol,⁴⁸ while $D([HCl]_2^+) = 20.1$ kcal/mol.⁴⁹ A simple diagrammatic explanation for this effect, Figure 12, invokes the interactions between the highest occupied molecular orbitals of the two partners. In qualitative molecular orbital theory the interaction is greater for orbitals of equal energy in $A \cdot A$ than it is for orbitals of unequal energy in $A \cdot B$. At the threshold for ionization an electron is removed from the antibonding orbital, leaving the ion with two bonding and one antibonding electrons, the net result being bonding. The greater interaction for $A \cdot A$ means that the net bonding of $(A \cdot A)^+$ is greater than it is for $(A \cdot B)^+$. Also, in view of this reasoning, the relatively small value we measured for $D([C_4H_8 \cdot SO_2]^+)$ no longer seems so surprising. In $(A \cdot A)^+$ the odd electron and net positive charge are delocalized equally over both partners while in $(A \cdot B)^+$ they remain localized mainly on A , so that one anticipates that $(C_4H_8 \cdot SO_2)^+$ has the structure $C_4H_8^+ \cdot SO_2$. Of course, in some cases chemical reaction between the two partners, such as occurs²⁵ with $(C_2H_4)_2^+$, overrides the above considerations.

The heterodimers studied in this work might be considered to be electron donor-acceptor complexes,^{40a} since sulfur dioxide has an appreciable electron affinity,⁵⁰ 1.08 ± 0.07 eV, while the ionization potentials of t - C_4H_8 and C_6H_6 are a relatively small 9.130 and 9.248 eV, respectively.¹¹ However ab initio calculations show that charge-transfer forces alone are inadequate to predict the properties of heterocomplexes.⁵¹ Morokuma⁵¹ has suggested, for convenience, a decomposition of energy contributions into five components: electrostatic interaction, polarization interaction, exchange repulsion, charge transfer, and a coupling term to take account of higher order interactions. The polarization interaction is also likely to be significant for t - $C_4H_8 \cdot SO_2$ and $C_6H_6 \cdot SO_2$, because sulfur dioxide has a sizable permanent dipole moment of 1.63 D.⁵² In contrast, since $(C_4H_8 \cdot SO_2)^+$ can reasonably be regarded as $C_4H_8^+ \cdot SO_2$, both electrostatic and polarization interactions should be expected to be much stronger for this ionic complex than for neutral t - $C_4H_8 \cdot SO_2$, contrary to our result, $D_0([C_4H_8 \cdot SO_2]^+) < D_0(t$ - $C_4H_8 \cdot SO_2)$. One possible explanation involves the structure of the ionic complex. If the neutral complex t - $C_4H_8 \cdot SO_2$ is such that the relatively positive sulfur atom is closest to the olefin and the negative oxygen atoms are farthest away, then when the olefin becomes suddenly ionized the SO_2 moiety would not necessarily have its most stable orientation. In that case complexes in the most stable configuration would not be formed by direct ionization because the Franck-Condon factors would be very small, but might still be formed weakly by the autoionization of discrete states, as evidently happens in the process⁴⁸ $C_6H_6 \cdot HCl + h\nu \rightarrow (C_6H_6 \cdot HCl)^+ + e$. However, there

(48) E. A. Walters, J. R. Grover, M. G. White, and E. T. Hui, *J. Phys. Chem.*, **89**, 3814-3818 (1985).

(49) P. W. Tiedemann, S. L. Anderson, S. T. Ceyer, T. Hirooka, C. Y. Ng, B. H. Mahan, and Y. T. Lee, *J. Chem. Phys.*, **71**, 605-609 (1979).

(50) (a) Weighted average of several measurements cited in B. K. Janousek and J. I. Brauman, "Gas Phase Ion Chemistry", Vol. 2, M. T. Bowers, Ed., Academic Press, New York, 1979, Chapter 10, pp 53-86; (b) J. J. Grabowski, J. M. Van Doren, C. H. DePuy, and V. M. Bierbaum, *J. Chem. Phys.*, **80**, 575-577 (1984); (c) G. Caldwell and P. Kebarle, *Ibid.*, **80**, 577-579 (1984).

(51) K. Morokuma, *Acc. Chem. Res.*, **10**, 294-300 (1977).

(52) R. D. Nelson, Jr., D. R. Lide, and A. A. Maryott, "Selected Values of Electric Dipole Moments in the Gas Phase", NSRDS-NBS 10, National Bureau of Standards, Washington, D. C., 1967.

(44) M. Meot-Ner (Mautner), *Acc. Chem. Res.*, **17**, 186-193 (1984).

(45) (a) M. Meot-Ner and F. H. Field, *J. Chem. Phys.*, **61**, 3742-3749 (1974); (b) M. Meot-Ner (Mautner), P. Hamlet, E. P. Hunter, and F. H. Field, *J. Am. Chem. Soc.*, **100**, 5466-5471 (1978); (c) M. Meot-Ner (Mautner), *J. Phys. Chem.*, **84**, 2724-2728 (1980).

(46) (a) P. M. Dehmer and S. T. Pratt, *J. Chem. Phys.*, **77**, 4804-4817 (1982); (b) S. T. Pratt and P. M. Dehmer, *Ibid.*, **78**, 6336-6338 (1983).

(47) (a) Y. Ono, E. A. Osuch, and C. Y. Ng, *J. Chem. Phys.*, **74**, 1645-1651 (1981); (b) Y. Ono, S. H. Linn, H. F. Prest, M. E. Gress, and C. Y. Ng, *Ibid.*, **73**, 2523-2533 (1980).

is no evidence for a region of structures due to autoionization below the obvious onset in the spectrum for the production of $(C_4H_8 \cdot SO_2)^+$ in Figure 5, so we assume that our reported value for $D_0([C_4H_8 \cdot SO_2]^+)$ corresponds to the ground state of the ionic complex.

There are a number of limitations to the technique described herein that must be acknowledged. (1) Normalization of the two spectra in preparation for subtraction requires that the threshold for photoionization of A be characterized by a distinctive feature. (2) The approximately linear threshold for dissociative photoionization of the dimer requires a step-function onset for photoionization of A. When the photoionization of A displays only a weak and indistinct onset, the present technique is inadequate. (3) Autoionization features in the threshold function for dissociative photoionization of the dimer could distort its linearity. (4) If $D(A \cdot B)$ is too small, the interval between the ionization potential of A and the appearance potential of A^+ from $A \cdot B$ becomes too narrow to allow the necessary normalization of the spectra to be carried out. This establishes a practical lower limit of roughly 1 kcal mol⁻¹ (0.04 eV) for dissociation energies that can be measured with our apparatus. It should be noted that dimers of this or lower dissociation energies can readily be made in useful densities by suitable adjustment of nozzle design and expansion conditions. (5) Optimization of the dimer density and minimization of the interference from trimers determines the beam temperature, so there is always a correction for the beam temperature in passing from the measured dissociation energy to the dissociation energy at 0 K, the uncertainty of which correction

increases the uncertainty that must be cited for the measurement. (6) As already discussed, if the target beam contains more than one isomer of the dimer in important amounts, the measured dissociation energy will likely be that of the least bound one. (7) The process $A \cdot B + h\nu \rightarrow A^+ + B + e$ must proceed with sufficiently large cross sections in the threshold region to allow its efficiency function to be resolved from the statistical scatter of measured points after the normalization and subtraction have been carried out. Our attempt to measure the dissociation energy of the benzene dimer was not successful because the cross sections are too small. As already explained above, small cross sections are to be expected whenever the dissociation energy of the dimer ion $(A \cdot B)^+$ is large, e.g., whenever $D([A \cdot B]^+) > 15$ kcal mol⁻¹. However, small cross sections can also occur for some other reason(s) that is(are) not yet understood. (8) Other potential problems that can be foreseen are effects due to ion pair formation, hot bands, delayed ion dissociation, and nonexistence of a stable A^+ (e.g. if $A = SF_6$).

Acknowledgment. We wish to thank the NSLS/HFBR Faculty-Student Support Program for travel funds to make this work possible. This research was carried out at Brookhaven National Laboratory under Contract DE-AC02-76CH00016 with the U.S. Department of Energy and supported by its Division of Chemical Sciences, Office of Basic Energy Sciences. We also thank E. T. Hui and P. F. Fernandez for assistance with the experiments. This work was performed while one of us (E.A.W.) was on sabbatical leave from the University of New Mexico.

Photodissociation of the Dimanganese Ion, Mn_2^+ : A Route to the Energetics of Metal Clusters

Martin F. Jarrold, Andreas J. Illies,[†] and Michael T. Bowers*

Contribution from the Department of Chemistry, University of California, Santa Barbara, California 93106. Received May 16, 1985

Abstract: The results of a study of the photodissociation of the dimanganese ion (Mn_2^+) in the visible region of the spectrum (477–590 nm) are reported. Experiments were performed using a crossed high-energy ion beam/laser beam apparatus. Photofragment relative kinetic energy distributions and angular distributions are reported. The kinetic energy distributions show two components which were assigned to ground and excited electronic state products. The angular distributions are characterized by an asymmetry parameter of $\beta = 0.4 \pm 0.1$ which indicates photodissociation does not occur via a direct transition to a repulsive excited state. The interpretation of kinetic energy thresholds in the photofragment distributions leads to a rigorous lower limit for the metal-metal bond energy of Mn_2^+ of $D^0_0(Mn^+ - Mn) \geq 1.39$ eV (32 kcal mol⁻¹) and an upper limit for the ionization potential of the neutral dimer of $IP(Mn_2) \leq 6.47$ eV.

I. Introduction

Metal clusters have been the subject of a rapidly expanding research effort over the past 2 or 3 years.¹⁻¹¹ Studies of metal clusters impact on a diverse range of both applied and fundamental research areas. These include catalysis and its relationship with studies of well-characterized surfaces as well as microelectronics and solid-state physics, particularly with regard to understanding the emergence of bulk properties such as metallic conductivity and band structure.

Metal clusters have been studied in matrices and in the gas phase. Recent interest has focused more on gas-phase studies, in part because of the inherent difficulty of the matrix studies.¹ However, studying metal clusters in the gas phase is not easy owing to the difficulty in generating the clusters. With the exception

of the alkali metals, most metals are refractory. Hence, high-temperature ovens² or pulsed laser evaporation³ are required to

(1) See, for example: Ozin, G. A., *Faraday Symp. Chem. Soc.* **1980**, 14. DiLella, D. P.; Limm, W.; Lipson, R. H.; Moskovits, M.; Taylor, K. V. *J. Chem. Phys.* **1982**, 77, 5263. Baumann, C. A.; Van Zee, R. J.; Weltner, W. *Ibid.* **1983**, 79, 5272. Bondybey, V. E.; English, J. H. **1980**, 72, 6479.

(2) Riley, S. J.; Parks, E. K.; Mao, C.-R.; Pobo, L. G.; Wexler, S. *J. Phys. Chem.* **1982**, 86, 3911.

(3) Dietz, T. G.; Duncan, M. A.; Powers, D. E.; Smalley, R. E. *J. Chem. Phys.* **1981**, 74, 6511. Bondybey, V. E. *J. Phys. Chem.* **1982**, 86, 3396.

(4) See, for example: Hopkins, J. B.; Langridge-Smith, P. P. R.; Morse, M. D.; Smalley, R. E. *J. Chem. Phys.* **1983**, 78, 1627. Bondybey, V. E.; Heaven, M.; Miller, T. A. *Ibid.* **1983**, 78, 3593. Bondybey, V. E.; English, J. H. *Ibid.* **1983**, 79, 4746. Morse, M. D.; Hopkins, J. B.; Langridge-Smith, P. P. R.; Smalley, R. E. *Ibid.* **1983**, 79, 5316.

(5) See, for example: Riley, S. J.; Parks, E. K.; Nieman, G. C.; Pobo, L. G.; Wexler, S. *J. Chem. Phys.* **1984**, 80, 1360. Geusic, M. E.; Morse, M. D.; Smalley, R. E. *Ibid.* **1985**, 82, 590. Whetten, R. L.; Cox, D. M.; Trevor, D. J.; Kaldor, A. *Ibid.* **1985**, 89, 566.

[†] Present address: Department of Chemistry, Auburn University, Auburn, AL 36849.